Peer-reviewed version available at Nanomaterials 2018, 8, 661; doi:10.3390/nano8090661

Type of the Paper (Review)

Tunable Metal-Organic Frameworks for Heat Transformation Applications

Somboon Chaemchuen[1,2], Xuan Xiao[2], Nikom Klomkliang[4], Mekhman S. Yusubov[1], Francis Verpoort[1,2,3,*]

[1] National Research Tomsk Polytechnic University, Lenin Avenue 30, 634050 Tomsk, Russian Federation.

[2] Laboratory of Organometallics, Catalysis and Ordered Materials, State Key Laboratory of Advanced Technology for Materials Synthesis and Processing; Center for Chemical and Material Engineering, Wuhan University of Technology, Wuhan 430070, P.R. China

[3] Ghent University, Global Campus Songdo, 119 Songdomunhwa-Ro, Yeonsu-Gu, Incheon, Korea

[4] School of Chemical Engineering, Suranaree University of Technology, Nakhon Ratchasima 30000, Thailand

***** Correspondence: Francis.verpoort@ugent.be/Francis.cn@qq.com

Abstract: Metal-Organic Frameworks (MOFs) are a subclass of porous materials that have unique properties such as varieties of structures from different metals and organic linkers, tunable porosity from a structure or framework design, etc. Moreover, modification/functionalization of the material structure could optimize the material properties and demonstrate high potential for a selected application. MOF materials exhibit exceptional properties and make these materials widely applicable including in energy storage and heat transformation applications. This review aims to give a broad overview of MOFs and their development as adsorbent materials having the potential for heat transformation applications. We summarize current investigations, developments, and possibilities of metal-organic frameworks (MOFs) especially the tuning of the porosity and hydrophobic/hydrophilic design required for this specific application. These materials applied as adsorbent are promising in the thermal driven adsorption for heat transformation using water as working fluid and related application.

Keywords: Metal-organic frameworks, heat transformation, low temperature heat, adsorbent, water adsorption

1. Introduction

The energy demand is steadily growing and becomes a worldwide issue, especially due to the continuous rise in energy consumption related to the increase in the world population. Moreover, the energy resources and exploration of new resources are limited and opposites with the worldwide energy demand. Including the environmental concerns, the development undertaken towards the exploration of environmentally friendly renewable energy is still challenging. Furthermore, nearly one-third of the worldwide energy is consumed for household usage for heat transformation (heating and cooling).[1] The demand for air-conditioned environment rapidly grows due to, higher living standards, increased climate temperatures as

well as architectural trends. Also, there is an increasing concern over ozone depletion and the global warming properties of applied compounds, e.g. CFCs and HFCs in household systems for heat transformation. In the meantime, the development and deployment of energy-saving and environmentally friendly technologies used for new heat transformation systems offer great potential to sustain and address the ever-increasing worldwide energy demand. Thermally driven adsorption chillers and adsorption heat pumps in heat transformation systems based on the reversible adsorption/desorption of the working fluid applying porous adsorbent materials are very promising. The more efficient use of low-temperature heat and an effective adsorption approach, as well as an effective climate protection through the reduction of the environmental impact of conventional heating and cooling devices, is encouraging. The main principle of the process is based on the consecutive adsorption/desorption processes.[2] Large advances in the enhancement of heat transformation performance can be achieved with the development of new adsorbent materials. Therefore current progress in this field is essentially related to the development of innovative materials which are properly adapted to this targets. Extensive research has been devoted to the design, synthesis, and development of new adsorbents with a water uptake capacity exceeding that of existing commercial materials (e.g., silicas or zeolites) and offering relatively milder regeneration conditions.

The micro- and mesoporous materials are significantly developed and exhibit potential for heat transformation systems used as adsorbent materials.[3] Nonetheless, most of the available adsorbents used for heat transformation systems have originally been developed for gas separation and catalysis.[4, 5] Silica gel or silica-aluminophosphates are the most reported adsorbent materials for heat transformation systems due to their advantageous high adsorption capacity of the working fluid which is mostly water. However, the working fluid (water) is mostly uptaken at a too high relative pressure which is the main problem to use the current adsorbent material *such as* silica. The resulting loading difference (in gram of adsorbed vapor/kilogram of adsorbent) of the adsorbent over a given cycle or cycle efficiency is small compared to the total adsorption capacity.[6] Therefore, there is an ongoing search for new materials with higher water uptake capabilities, required to improve the system performance of a heat transformation system. In this respect, new materials such as metal-organic frameworks (MOFs) generated from metal ions/clusters bridging with organic linkers have a great perspective as an adsorbent to replace currently applied adsorbents. During recent decade, these materials have witnessed a booming development and burgeoning in various potential applications such as gas adsorption and storage, separation, catalysis, sensing, *etc.*[7-9] As their structures can be constructed of a diversity of metal clusters/ions and organic components and generating porous materials with a high surface area, MOFs possess more advantages to tune their properties via structure design. Moreover, the modification of MOFs *via* functionalization or post-synthetic modification could offer attractive routes to enhance their properties for heat transformation and related applications.

2. Heat transformation systems

Preprints (www.preprints.org) | NOT PEER-REVIEWED | Posted: 13 July 2018 doi:10.20944/preprints201807.0242.v1

Peer-reviewed version available at Nanomaterials 2018, 8, 661; doi:10.3390/nano8090661

The thermodynamic principle of a heat transformation system using a solid adsorbent with the work produced by the heat engine driving the heat pump cycle is illustrated in Figure 1. Basically, an ideal cycle in heat transformation application consists of two processes between a vapor (working fluid) adsorption on highly porous solid materials (adsorbent) followed by the regeneration or desorption cycle. In the adsorption cycle, the working fluid is evaporated with heat at a low-temperature level, thereby producing the beneficial cooling. When the vapor is adsorbed on the porous solid, it releases the adsorption heat at a medium temperature level which can be used as a useful heat in the heat pump case or withdrawn to the environment in case of the cooling applications. As the adsorption is an exothermic process, the adsorbent extracts heat from the evaporator and produce a cooling effect. Later, during the regeneration or desorption cycle, heat from a high-temperature source (e.g., solar thermal collector, gas burner) is used to desorb the vapor from the porous solid. The released water vapor condenses at a medium temperature level (ambient temperature) with the heat of condensation released into the environment. As desorption is an endothermic process, it helps to release the refrigerant (water vapor) from the hot bed. After that, the hot refrigerant will be cooled in a condenser to feed the evaporator with the refrigerant liquid and the cooling process is maintained in a continuous manner.

In a standard process, the sorption system exchanges the fluid vapor (evaporator/condenser) between the liquid phase and the adsorbent material. The working fluid is important in the process since it has a specific evaporation enthalpy. Preferable water is applied as a working fluid, however, other fluids such as ethanol, methanol, acetone, etc., also can be used for specific purposes. Nevertheless, adsorbent materials are most important regarding the process efficiency to adsorb vapor of the working fluid and highly porous solid materials such as MOFs exhibit this property.

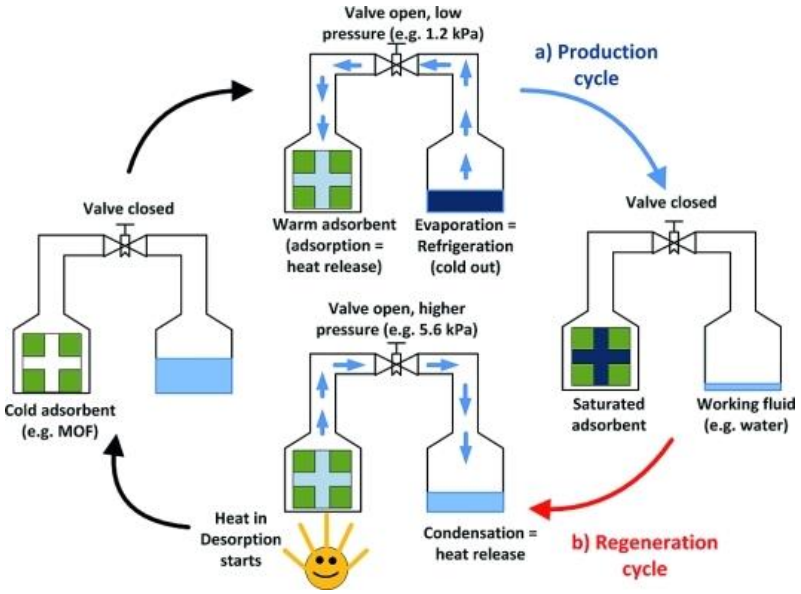

Preprints (www.preprints.org) | NOT PEER-REVIEWED | Posted: 13 July 2018 doi:10.20944/preprints201807.0242.v1

Peer-reviewed version available at Nanomaterials 2018, 8, 661; doi:10.3390/nano8090661

Figure 1. Illustration of the basic principle for adsorption chillers or heat pumps. (Reproduced with permission from ref. [10])

Desalination is generally defined as the heat transformation process by which potable water is produced from seawater or brackish water with a high dissolved suspended solid content (35,000 ppm). Desalination processes can be divided into two major groups: the first group is a heat-driven process (distillation) such as multi-stage flashing (MSF), multiple effect distillation (MED) and solar distillation. The second group employs electric power driven processes that include freezing, mechanical vapor compression, electrodialysis and reversed osmosis. All the desalination systems suffer from two drawbacks namely; high energy intensive and/or prone to fouling and corrosion of the evaporator or separation unit of the sea water.[11] Recently, a new process of adsorption desalination using adsorbent has been identified with many advantages such as environmentally friendly, driven by low-grade heat sources, low capital cost, low evaporation temperature and hence reduced fouling (formation of scales causing the damage of the evaporation units) effect. The adsorption system consists of an evaporator, a condenser and adsorption/desorption beds. Each bed includes a finned tube heat exchanger with the adsorbent material packed between the fins. The process starts with the evaporation of seawater producing a water vapor which is then adsorbed by the adsorbent material. Then during the desorbing step where the bed is heated, the water vapor is released and then condensed in the condenser producing high grade distilled water (Fig.2).[12] Different adsorbent materials such as silica-gel and zeolite have been reported for the desalination application.[13-15]

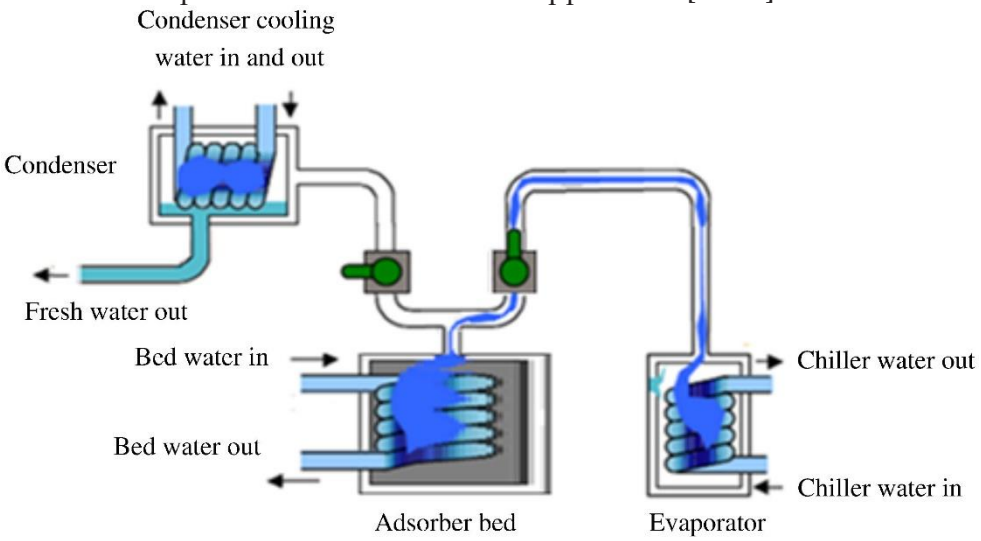

Figure 2. Schematic diagram for a one-bed adsorption desalination. (Reproduced with permission from ref.[12])

3. Metal-organic frameworks as adsorbent materials

It is clear that adsorbent materials are key in the development of heat transformation technologies. In this respect, the discovery of new materials applicable for adsorption-desorption working fluid is still a fundamental research of which the development of this technology is ongoing.[16-19] Porous coordination polymers (PCPs) also well known as metal-organic frameworks (MOFs) demonstrated excellent properties as adsorbent and are explored for heat transformation applications. Due to their huge surface (having micro- to macro-pores), chemical and physicochemical variability tunable composition/properties can be designed. Moreover, MOFs consist of both hydrophilic and hydrophobic moieties in the same structure which possess some unique adsorption properties. Compared with a vast number of natural and synthetic adsorbents, MOF materials have a high potential for heat transformation applications because of their high ability in adsorption of guest molecules, including water (working fluid), and thermal stability.[16, 20] Additionally, MOFs possessing hydrophilic properties have an advantage over silica gel, they exhibit a non-limited water uptake at high relative pressure values reaching their maximum capacity. Initially, the demonstration of MOFs as adsorbent materials was carried out by investigating the capability of solid-gas adsorption applications for energy transformation. The energy storage and heat transformation (cooling/heating) using MOFs materials proved to have great potential applications. The investigated adsorbent materials were characterized via water adsorption-desorption properties since water is mostly used as a working fluid. In addition, MOFs have been considered for water adsorption measurements in order to investigate the structural properties and adsorption performances. For some frameworks, a geometric flexibility and reversible change in the structure related to the guest adsorption was observed. Consequently, the water adsorption on MOFs was used to evaluate their performance for heat transformation application.

Compared to traditional adsorbents used in heat pump applications, like zeolites or aluminophosphates, MOFs exhibit a much richer variety in terms of composition, pore structure, and topology. Moreover, it is also possible to modify the metal clusters/ions and organic linkers, as well as the porous structure of the MOFs allowing the tuning of their adsorption properties.[21] This opens attractive prospects for the design of MOFs with predetermined properties adopted for operating conditions particular suitable heat transformations.[20] Remarkably, advances in MOF chemistry have permitted the deployment of several strategies for the synthesis and modification of water-stable MOFs, paving the way for water-sorbent candidates for water adsorption-related applications (Table 1).[22-26] From a qualitative point of view, the adsorption properties of MOFs are obviously quite diverse in terms of water uptake capacity and the associated relative pressure at which the pore filling occurs. Certainly, hydrolytically stable porous materials offering remarkable pore volumes are expected to exhibit large water adsorption capacities. The quest for hydrolytically stable and recyclable MOFs with superior total water uptake remains a focal point of intensive research in the MOF chemistry.

Table 1. Summary potential MOFs and their properties in water adsorption (Reproduced with permission from ref. [23])

Preprints (www.preprints.org) | NOT PEER-REVIEWED | Posted: 13 July 2018 doi:10.20944/preprints201807.0242.v1

Peer-reviewed version available at Nanomaterials 2018, 8, 661; doi:10.3390/nano8090661

MOFs	Metals	Linkers	Surface area ($m^2 \cdot g^{-1}$)	Pore diameter (nm)	Pore volume ($cm^3 \cdot g^{-1}$)	Uptake* ($cm^3 \cdot g^{-1}$)	ref.
CAU-10	Al	1,3-H_2BDC	635	0.7	0.25	0.31	[27]
CAU-10-H	Al	1,3-H_2BDC	635	n.d.	0.5	0.382	[27]
CAU-10-NH_2	Al	5-H_2BDC-NH_2	n.d.	n.d.	n.d.	0.19	[27]
CAU-10-NO_2	Al	5-H_2BDC-NO_2	440	n.d.	0.18	0.15	[27]
CAU-10-OCH_3	Al	5-methoxyiso-phthalic acid	n.d.	n.d.	n.d.	0.07	[27]
CAU-10-OH	Al	5- H_2BDC-OH	n.d.	n.d.	n.d.	0.27	[27]
CAU-6	Al	BDC- NH_2	620	n.d.	0.25	0.485	[28]
DUT-4	Al	H_2NDC	1360	n.d.	0.79	0.28	[29]
DUT-67	Zr	H_2TDC	1560	1.66/0.88	0.60	0.625	[30]
MIL-100	Cr	H_3BTC	1517	2.5/2.9	n.d.	0.41	[31]
MIL-100	Fe	H_2BDC	1549	n.d.	0.82	0.81	[29]
			1917	2.5/2.9	1.0	0.77	[32]
MIL-100	Al	H_3BTC	1814	2.5/2.9	1.14	0.50	[32]
MIL-100	Cr	H_3BTC	1330	2.5/2.9	0.77	0.40	[33]
			2059	2.9/3.4	1.103	1.01	[34]
			3017	n.d.	1.61	1.28	[29]
			3124	2.9/3.4	1.58	1.40	[35]
MIL-100-DEG	Cr	H_3BTC	580	1.2/1.5/1.9	0.50	0.33	[33]
MIL-100-EG	Cr	H_3BTC	710	1.2/1.5/1.9	0.47	0.43	[33]
MIL-101-NH_2	Cr	H_2BDC	2509	<2.9/3.4	1.27	0.90	[35]
			2690	<2.9/3.4	1.60	1.06	[36]
MIL-101-NO_2	Cr	H_2BDC	2146	<2.9/3.4	1.19	1.08	[35]
			1245	<2.9/3.4	0.7	0.44	[36]
MIL-101-*p*NH_2	Cr	H_2BDC	2495	<2.9/3.4	1.44	1.05	[36]
MIL-101-*p*NO_2	Cr	H_2BDC	2195	<2.9/3.4	1.11	0.6	[36]
MIL-125	Ti	H_2BDC	1160	0.6/1.1	0.47	0.36	[37]
MIL-125-NH_2	Ti	H_2BDC-NH_2	830	0.6/1.1	0.35	0.36	[37]
			1220	0.6/1.26	0.55	0.37	[38]
MIL-53	Al	H_2BDC	1040	0.7-1.3	0.51	0.09	[37]
			n.d.	n.d.	n.d.	0.09	[39]
MIL-53-NH_2	Al	H_2BDC-NH_2	940	0.7-1.3	0.37	0.05	[37]
			n.d.	n.d.	n.d.	0.09	[39]
MIL-53-OH	Al	H_2BDC-OH	n.d.	n.d.	n.d.	0.40	[39]
MIL-53	Ga	H_2BDC	1230	0.8-2	0.47	0.05	[37]
MIL-53-NH_2	Ga	H_2BDC-NH_2	210	0.8-2	n.d.	0.02	[37]
MIL-53-$(COOH)_2$	Fe	H_2BDC-$(COOH)_2$	n.d.	n.d.	n.d.	0.16	[39]
MIL-68	In	H_2BDC	1100	0.6/1.6	0.42	0.32	[37]
MIL-68-NH_2	In	H_2BDC-NH_2	850	0.6/1.6	0.302	0.32	[37]
MOF(NDI-SEt)	Zn	Pyrazole ligands	888	n.d.	1.6	0.25	[40]

Preprints (www.preprints.org) | NOT PEER-REVIEWED | Posted: 13 July 2018 doi:10.20944/preprints201807.0242.v1

Peer-reviewed version available at *Nanomaterials* **2018**, *8*, 661; doi:10.3390/nano8090661

MOFs	Metals	Linkers	Surface area ($m^2 \cdot g^{-1}$)	Pore diameter (nm)	Pore volume ($cm^3 \cdot g^{-1}$)	Uptake* ($cm^3 \cdot g^{-1}$)	ref.
MOF(NDI-SO_2Et)	Zn	Pyrazole ligands	764	n.d.	<1.6	0.25	[40]
MOF(NDI-SOEt)	Zn	Pyrazole ligands	927	n.d.	<1.6	0.30	[40]
MOF-199	Cu	H_3BTC	1340	n.d.	0.72	0.55	[29]
			921	2.1	0.492	0.64	[41]
			1270	0.9,0.6	0.62	0.49	[42]
MOF-74	Co	DOT	1130	1.11	0.49	0.63	[30]
MOF-74	Mg	DOT	1250	1.11	0.53	0.75	[30]
			1400	1.1	0.65	0.62	[42]
MOF-74	Ni	DOT	1040	1.11	0.46	0.615	[30]
			639	2.3	0.362	0.48	[41]
MOF-801-P	Zr	Fumaric acid	990	0.74,0.56,0.48	0.45	0.450	[30]
MOF-801-SC	Zr	Fumaric acid	690	0.74,0.56,0.48	0.27	0.35	[30]
MOF-802	Zr	PZDC	1290	0.84,0.74	0.49	0.11	[30]
MOF-804	Zr	DOT	1145	0.72,0.68	0.46	0.29	[30]
MOF-805	Zr	NDC-$(OH)_2$	1230	0.95,0.86	0.48	0.415	[30]
MOF-806	Zr	BPDC-$(OH)_2$	2220	1.26,1.01	0.85	0.425	[30]
MOF-808	Zr	BTC	2060	1.84	0.84	0.735	[30]
MOF-841	Zr	H_4MTB	1390	0.92	0.53	0.640	[30]
PIZOF-2	Zr	PEDB-$(OMe)_2$	2080	1.76	0.88	0.850	[30]
SIM-1	Zn	4-methyl-5-imidazolecarboxaldehyde	570	0.65	0.303	0.14	[37]
UiO-66	Zr	H_2BDC	1290	0.84,0.74	0.49	0.535	[30]
			1032	0.75/1.2	0.77	0.40	[38]
			1105		0.55	0.39	[43]
			1160	0.6	0.52	0.37	[42]
UiO-66-1,4-Naphyl	Zr	1,4-Naphyl	757	n.d.	0.42	0.26	[43]
UiO-66-2,5-$(OMe)_2$	Zr	2,5-$(OMe)_2$	868	n.d.	0.38	0.42	[43]
UiO-66-NH_2	Zr	H_2BDC-NH_2	1328	0.75/1.2	0.70	0.38	[38]
			1123	<0.75/1.2	0.52	0.34	[43]
			1040	0.6	0.57	0.37	[42]
UiO-66-NO_2	Zr	H_2BDC-NO_2	792	<0.75/1.2	0.40	0.37	[43]
UiO-67	Zr	H_2BPDC	2064	1.2/1.6	0.97	0.18	[38]
ZIF-8	Zn	2-MIM	1255	n.d.	0.64	0.02	[29]
			1530	1.1	0.485	0.01	[37]

*Water adsorption properties measured at 298 K at nearly saturated vapor pressure ($P/P_0 \approx 1$), n.d. = non data,
Ligand abbreviation: 1,3-H_2BDC = 1,3-benzenedicarboxylic acid / 1,4-Naphyl = 1,4-naphthalenedicarboxylic acid / 2,5-$(OMe)_2$ = 2,5-dimethoxy-terephthalic acid / 2-MIM = 2-methylimidazole / 5- H_2BDC-NH_2 = 5-aminoisophthalic acid / 5-H_2BDC-NO_2 = 5-nitroisophthalic acid / 5- H_2BDC-OH = 5-hydroxyisophthalic acid / DEG = diethylene glycol / DOT or

Preprints (www.preprints.org) | NOT PEER-REVIEWED | Posted: 13 July 2018 doi:10.20944/preprints201807.0242.v1

Peer-reviewed version available at Nanomaterials 2018, 8, 661; doi:10.3390/nano8090661

H_2BDC-$(OH)_2$= 2,5-dihydroxy-1,4-benzenedicarboxylic acid / EN = ethylenediamine / H_2BDC = 1,4-benzenedicarboxylic acid / H_2BDC-$(COOH)_2$ = 1,2,4,5-benzenetetracarboxylic acid / H_2BDC-NH_2= 2-aminoterephthalic acid / H_2BDC-NO_2= 2-nitro-terephthalic acid / H_2BDC-OH = 2-hydroxyterephthalic acid / H_2BPDC = biphenyl-4,4´-dicarboxylic acid / H_2BPDC-$(OH)_2$= 3,3'-dihydroxy-4,4'-biphenyldicarboxylic acid / H_2NDC-$(OH)_2$ =1,5-dihydroxynaphthalene-2,6-dicarboxylic acid / H_2-PEDB-$(OMe)_2$= 4,4'-[(2,5-dimethoxy-1,4-phenylene)bis(ethyne-2,1-diyl)]dibenzoic acid / H_2PZDC = 1H-pyrazole-3,5-dicarboxylic acid / H_2TDC = thiophene-2,5-dicarboxylic acid / H_3BTC = 1,3,5-benzenetricarboxylic acid / H_4MTB = 4,4',4'',4'''-methanetetrayltetrabenzoicacid.

The most common energy transformation is the sensible heat storage and latent storage. A higher thermal storage efficiency via increasing the thermal storage capacity (sensible heat capacity) is required to lower the volume of a sensible thermal storage system. Whereas, the working fluid based on water applying for heat storage and transformation has the highest mass-based evaporation enthalpy (2440 kJ/kg at 25 °C) and an adsorption enthalpy comparable to all known fluids.[44] To investigate a suitable candidate adsorbents were measurement via adsorption equilibrium data points corresponding to common cycle conditions (at the end of the adsorption and desorption half-cycle). The results demonstrated the outstanding performance of MOFs compared to silica gel and several zeolites (Figure 3).[44] Figure 3 displays that at a higher desorption temperature of 140 °C against a lower condensation pressure of 12 hPa (total height of the bars), the loading spread achieved with the new material MOF (ISE-1) amounts to ~210 g/kg and is larger compared with all five zeolites and the reference silica gel. To date, several MOFs have been suggested as water and methanol adsorbents for heat transformation system, see Figure 4, such as MIL-101[45], MIL-100, mp-AF or Basolite™ A520[46], NH_2-MIL-125[47], UiO-66[38], etc. This review aims to provide promising MOF-candidates with a special focus on sorption processes, based on the evaluation of the water uptake characteristics.

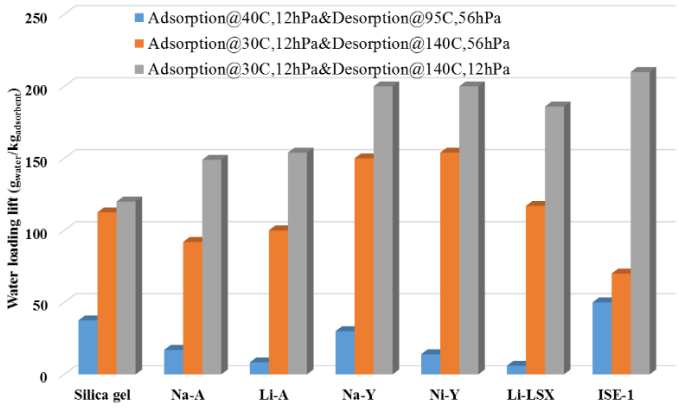

Figure 3. Water loading spread over the cooling cycle for various adsorbents. (Reproduced with permission from ref.[44])

Thermodynamic boundaries of MOFs adsorbent

The adsorption equilibria and the applied adsorption material are used to illustrate the heat transformation cycles. The first state of merit is the achievable working fluid (water) loading

Preprints (www.preprints.org) | NOT PEER-REVIEWED | Posted: 13 July 2018 doi:10.20944/preprints201807.0242.v1

Peer-reviewed version available at Nanomaterials 2018, 8, 661; doi:10.3390/nano8090661

on adsorbent materials, more precisely the working fluid exchange between the production cycle (adsorption) and the regeneration cycle (desorption). Using the van 't Hoff diagram in Figure 4 the exchange as the difference between the richest and the weakest isosteric of the cycle based on MOFs adsorbent can be described.[34] The minimum adsorption (point B) and the maximum desorption temperature (point D) by the evaporator and condenser pressure were used to determine the process, while in the thermodynamic context, the isosteric term occurs at a constant water loading without adsorption or desorption. In case of the cooling application (A→B), the water is evaporated and heat is adsorbed from the environment producing the useful chilling (cooling case). The cooling enthalpy produced in one cycle can be calculated simply as the evaporation enthalpy times the working fluid exchange. In the meantime, the heat of adsorption is released to the environment (in case of a heat-pump application) which is the useful heat. The cycle is defined by the highest desorption temperature (driving temperature, point D), the minimum adsorption temperature (point B), and the condenser and evaporator pressure. During isosteric heating (B→C), the pressure level increases to the condensation pressure level, thereby the selected pressure level is geared to the possible applications. Then, the saturated adsorption on the adsorbent material was regenerated (C→D), the heating from a high-temperature source (e.g. solar-thermal collector, waste heat) is used to desorb the working fluid from the adsorbent material. Finally, the isosteric cooling (D→A) closes the cycle. In an ideal cycle, adsorption and desorption are supposed to be an isobaric process. Hence the evaluation of materials for this type of application is realized by measurement of two isobars corresponding to the condenser and evaporator pressure.

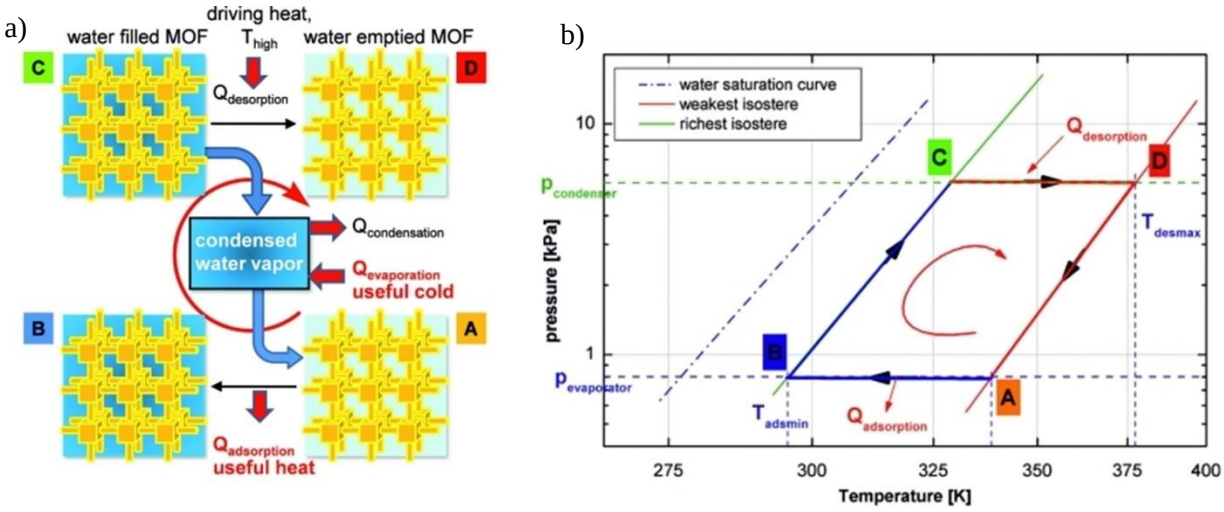

Figure 4. Principle process of the ideal cycle in an adsorption heat-pump or chiller process a) and diagram b). A→B: production or adsorption cycle. C → D: regeneration or desorption cycle (Reproduced with permission from ref.[10, 34])

Copper metal based MOFs

Preprints (www.preprints.org) | NOT PEER-REVIEWED | Posted: 13 July 2018 doi:10.20944/preprints201807.0242.v1

Peer-reviewed version available at Nanomaterials 2018, 8, 661; doi:10.3390/nano8090661

HKUST-1 or $Cu_3(BTC)_2$ is the most frequently investigated MOF for a variety of applications. Chui et al. were the first to produce a copper (Cu^{2+}) metal clusters bridging with a benzene-1,3,5-tricarboxylate linker (BTC).[48] HKUST-1 contains an intersecting 3-D system of large square shaped pores of 9 × 9 Å and other smaller pores having a diameter of 6 Å. In the framework of HKUST-1, Cu (II) ions form dimmers, where each copper atom is coordinated by four oxygens from the BTC linkers and water molecules. Moreover, HKUST-1 was the first available MOF having outstanding properties among the commercial available MOFs as shown by the interesting properties such as gas storage, gas separation, catalytic performance, *etc.*[49, 50] HKUST-1 demonstrated also an impressive performance in water adsorption of about 95-120 $g_{water}/kg_{adsorbent}$ at 40°C/ 1.2 kPa and 324 $g_{water}/kg_{adsorbent}$ at 30°C/ 1.2kPa which is much higher than the currently used adsorbents such as silica gel (Fig.5a). The presence of water molecules in the first coordination sphere of Cu ions has been suggested as a possible reason to obtain a coordinative vacancy on Cu (II) species. The second step in the adsorption isotherm either indicates the consecutive complete filling of the large pores or the filling of the smaller pores, which are of a more hydrophobic character, as they do not have any accessible metal sites. Additionally, the hydrophobic character of the benzene linker enhances the hydrophobicity of the small pores. They are less hydrophilic as the pore interior is constituted by four benzene rings.[51] A saturation is attained at about $p/p_0 = 0.4$. An additional increase of $p/p_0 = 0.9$-1.0 may result from the condensation of H_2O in the inter-particulate volume. The desorption exhibits a slight hysteresis due to strong hydrogen bonds formed between the water molecules.[16] Note that not all water molecules are desorbed in the lower pressure region. This phenomenon is probably the result of the chemisorption of water molecules on the free copper coordination sites. It is noteworthy that the pre-treatment and different preparation procedures (solvent used, crystal size, etc.) also affect the performance of adsorption. Unfortunately, the HKUST-1 is significantly unstable during its recycling experiment.

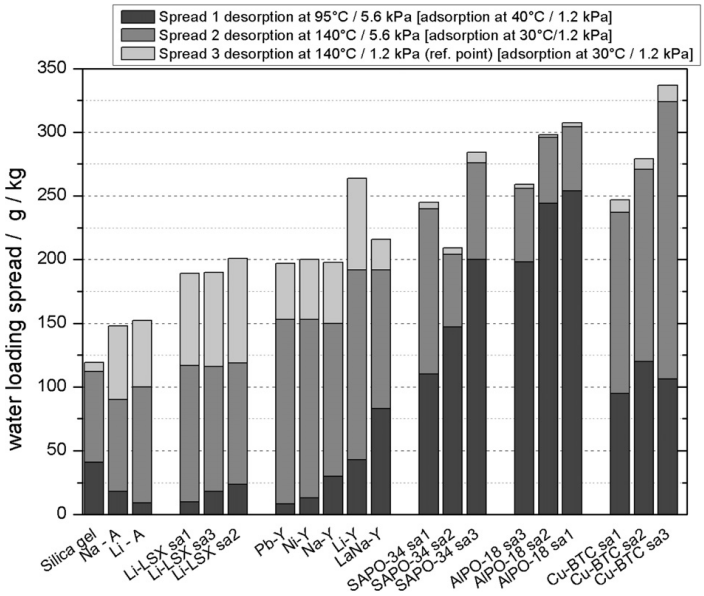

Figure 5. Comparison of water loading spread over three cycle conditions for different materials (Reproduced with permission from ref.[16])

MOF materials having a pillared-layer structure using Cu^{2+}, Na_2pzdc (pzdc=pyrazine-2,3-dicarboxylate), and a series of pillar ligands of pyridine derivatives were synthesized by Kitagawa[52] The structure of $Cu_2(pzdc)_2(dpyg)]_n$ (pzdc= pyrazine-2,3-dicarboxylate; dpyg=1,2-di(4-pyridyl)glycol) with a flexible and functional pillar were examined for the adsorption of CH_4, MeOH, and H_2O.[52] The MeOH adsorption isotherm displays a sudden rise at relative pressure (P/P_o) 0.23 and attains a saturated level (ca. 6.2 mmol/g) at point $P/P_o = 0.5$. On the other hand, the desorption isotherm does not follow the adsorption isotherm, instead, it shows an abrupt drop at $P/P_0 = 0.1$. Moreover, this hysteretic profile between the adsorption and desorption isotherms was reproducible for many times. The sharp adsorption jump/desorption drop within the hysteresis loop indicates the occurrence of a framework transformation in the crystal state, which should permit guest inclusion. This effect is mainly associated with the hydrogen bond interaction between the MeOH molecules and the OH groups of the dpyg ligands; the attractive force should be strong enough to transform the channel structure to allow the incorporation of the guest molecules. The use of a pillared layer motif for the rational synthesis based on the response of the flexible and dynamic framework to specific guest molecules opens up a new field in porous coordination materials.

Chromium (Cr) based MOFs

MILs (acronym for Matérial Institute Lavoisier) are chromium-based metal-organic frameworks that are extensively been investigated. Férey et al. were the first to synthesize and report the chromium-terephthalate-based solid (MIL-101).[53] The structure is built up from a Cr octahedral with rigid carboxylate ligands (terephthalate or trimesate) generating microporous super-tetrahedral units (Fig. 6). The connection of these motifs provides an augmented version of the 3D MTN zeolite topology.[54] The resulting cubic cell volumes are huge (~380,000 and 702,000 Å), with two types of porous cages limited by pentagonal faces for the smaller cage and by pentagonal and hexagonal faces for the larger cage. After removal of the guest molecules, the free internal diameters are close to 2.5 and 2.9 nm (MIL-100) and 2.9 and 3.4 nm (MIL-101). The cages are accessible through microporous windows of 0.55 and 0.86 nm (MIL-100) and 1.2 and 1.6 nm (MIL-101).[55] The MIL-101 showed exceptional properties such as high pore volume (2 cm^3/g), large surface area (4500 m^2/g), and water stable, high thermal stability etc.[56] Water adsorption/desorption was measured at 25°C which exhibited the adsorption *type IV* isotherm (Fig.7a). The adsorption mechanism revealed that the water vapor adsorption is related to the unsaturated metal center (UMCs) at low relative pressure ($P/P_o < 0.4$). Nevertheless, the hydrophobic properties of the ligand of the MOF prohibited further water uptake. At higher relative pressure (P/P_o = 0.4-0.5) a steep increase in water uptake was found due to the involvement of capillary condensation in the mesopores. At higher relative pressure ($P/P_o > 0.5$) a stable water uptake was observed as a result of the full filling of the pores with water. Since most adsorption occurs in the large pores of the material a hysteresis loop between the adsorption and desorption branches of the adsorption isotherms is obtained. Furthermore, the material

Preprints (www.preprints.org) | NOT PEER-REVIEWED | Posted: 13 July 2018 doi:10.20944/preprints201807.0242.v1

Peer-reviewed version available at Nanomaterials 2018, 8, 661; doi:10.3390/nano8090661

demonstrated a high hydrothermal stability since over 20 adsorption/desorption cycles could be performed successfully (Fig.7b).

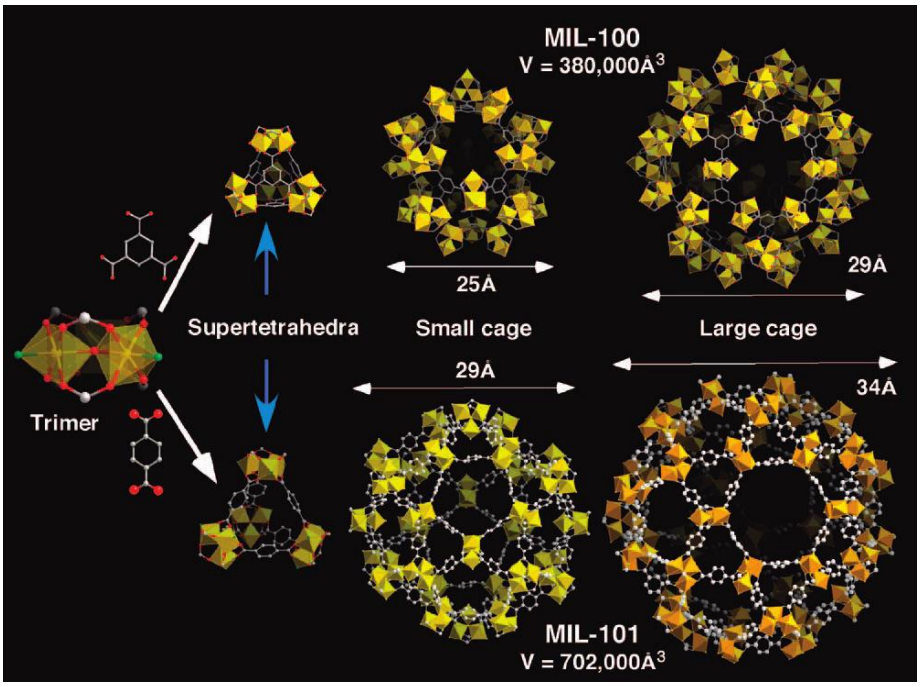

Figure 6. Structures of MIL-100 and MIL-101. (Reproduced with permission from ref. [57])

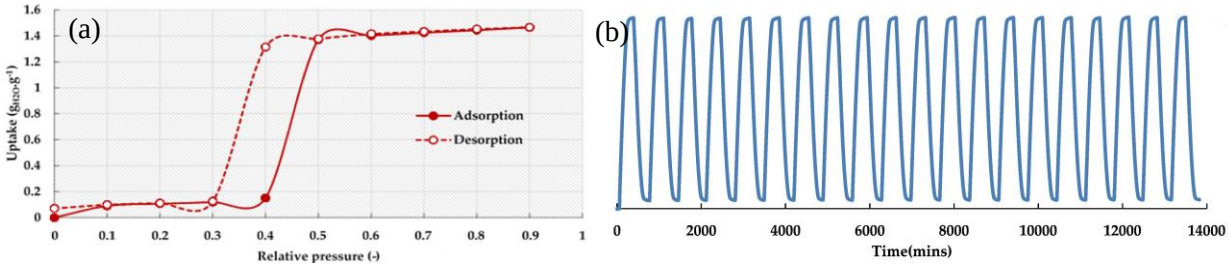

Figure 7. a) Water adsorption isotherms of MIL-101 at 25°C, b) Adsorption/desorption performance of MIL-101(Cr) at 25°C. (Reproduced with permission from ref. [58])

Nickel (Ni) based MOFs

MOF-74(Ni) also known as CPO-21-Ni (CPO: Coordination Polymer of Oslo) is a hydrothermally stable metal-organic framework.[59] The crystal structure of the CPO-27 is based on a honeycomb motif with pores of 12 Å diameter and helical chains of edge-condensed metal oxygen coordinated octahedra located at the intersections of the honeycomb. The water adsorption was performed on the material at 25°C and the obtained result exhibit a maximum

Preprints (www.preprints.org) | NOT PEER-REVIEWED | Posted: 13 July 2018 doi:10.20944/preprints201807.0242.v1

Peer-reviewed version available at Nanomaterials 2018, 8, 661; doi:10.3390/nano8090661

uptake of 0.47 $g_{water}/g_{adsorbent}$ at a relative pressure of 0.9 (Fig. 8). Noteworthy is that it has been reported that the water adsorption at low-pressure values is related to unsaturated metal centers (UMCs).[60] UMCs were formed after the removal of guest molecules on the metal atoms and these UMCs can easily attract water molecules via these extra binding sites. Moreover, the presence of a hydroxyl group on the organic linker, a hydrophilic advantage, is also involved in this phenomenon. On the other hand, the strong interaction on the binding sites with the guest molecules requires strong conditions for the regeneration process. In order to evaluate the performance stability, adsorption/desorption experiments were conducted using CPO-27(Ni) demonstrating an excellent performance stability during ten cycles with a negligible decrease (0.35%).

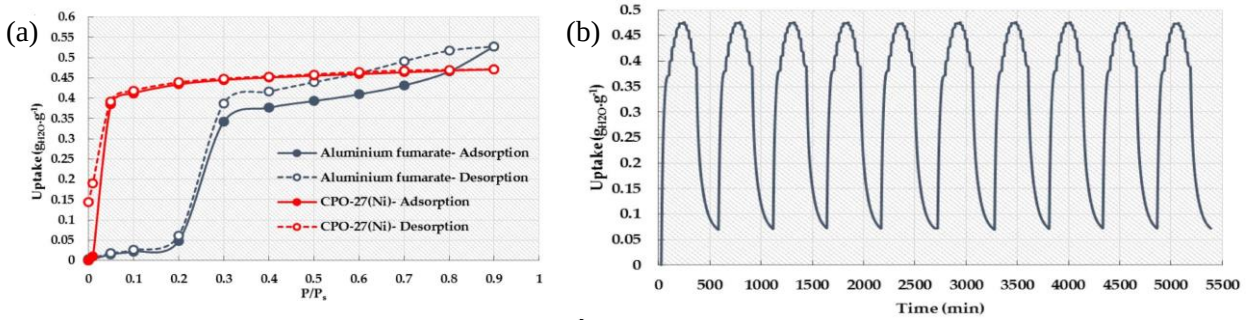

Figure 8. a) Water adsorption isotherms of CPO-27(Ni) at 25°C and b) Adsorption/desorption cycling experiments for CPO-27(Ni). (Reproduced with permission from ref.[60])

Aluminum (Al) based MOFs

Aluminum bridged with fumaric acid (FA) as an organic linker formed the MIL-53(Al)-FA structure having the formula Al(OH)(fum)·xH$_2$O (x=3.5; fum = fumarate) and exhibits an isoreticular structure to the well-known material MIL-53(Al)-BDC or Al(OH)(BDC) ·H$_2$O (BDC=1,4-benzenedicarboxylate). The framework is constructed from chains of corner-sharing metal octahedra linked together by fumarate to form lozenge-shaped 1D pores having circa 5.7 x 6.0 Å free dimensions. As expected, these sizes are smaller than those observed for the parent terephthalate open forms (7.3 x 7.7 Å for MIL-53(Al)-BDC (as-synthesized) and 8.5 x 8.5 Å MIL-53(Al)-BDC (at high temperature), consistent with the shorter length of the fumaric acid compared to the terephthalic acid.[61, 62] The water uptake in this material reached 0.53 $g_{water}/g_{adsorbent}$ at P/P_0= 0.9 (Fig. 8a). The adsorption isotherm exhibited a *type IV* isotherm with a hysteresis indicating a narrow distribution of uniform pores. The limited water adsorption at low relative pressure (P/P_0 < 0.2) is related relatively to the hydrophobic properties of the organic linker.[63] The steep increase in the water uptake at P/P_0 = 0.2 - 0.3 is followed by a continuous increase till the maximum adsorption is reached. The adsorption mechanism for the uniform accumulation of water molecules in the inner pores of the material has been reported as well.[59] It followed that a higher relative pressure is required to induce pore filling with water vapor.[63] The water adsorption/desorption cycles were performed and showed a steep decrease during the first four cycles followed by a stabilization of the adsorption/desorption up to 10 cycles (Fig.9).[60]

Preprints (www.preprints.org) | NOT PEER-REVIEWED | Posted: 13 July 2018 doi:10.20944/preprints201807.0242.v1

Peer-reviewed version available at Nanomaterials 2018, 8, 661; doi:10.3390/nano8090661

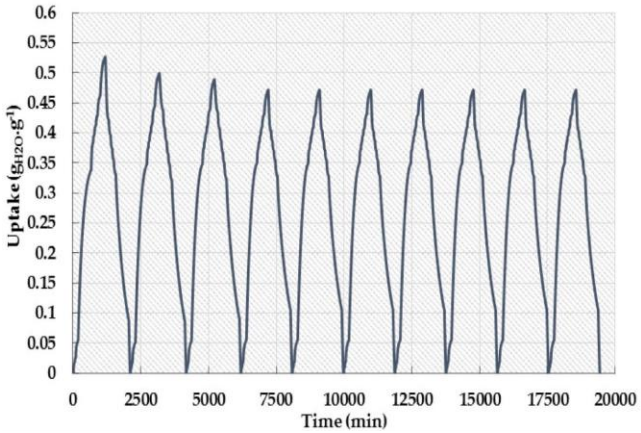

Figure 9. The adsorption/desorption experiments for aluminum fumarate. (Reproduced with permission from ref.[60])

CAU-10-H is one of the commercial MOFs that contains isophthalic acid as an organic linker and cis-connected AlO_6-polyhedra, forming helical chains. The potential of CAU-10-H is further strengthened by the fact that this material demonstrates a higher volumetric adsorption capacity and thermodynamic efficiency for water.[64] The highly pure crystalline phase is perfectly stable towards water and has not shown any sign of degradation over seven hundred repeated adsorption/desorption cycles, a feature not commonly encountered for MOFs when exposed to water.[65] The water adsorption isotherm shows the required *S*-shape with a steep rise at P/P_0 = 0.2 and a maximum uptake of approximately 0.33 $g_{water}/g_{adsorbent}$ and nearly no hysteresis. The material shows a structural transition indicating a flexibility of the material through adsorption and desorption, the so-called breathing effect.[65] Despite or because of this flexibility CAU-10-H is stable over 10,000 cycles of adsorption/desorption. The unique shape of the isotherms allows the use of very low desorption temperatures of less than 75°C at condensation temperatures around 30°C.[66]

MIL-100 with the empirical formula 3D-$(Al_3(btc)_2 \bullet nH_2O)$ (btc = benzene-1,3,5-tricarboxylate, trimesate) has received plenty of interest in the field of catalysis, gas separation and gas storage.[67-69] Water adsorption behavior was obtained at small relative pressures (P/P_0 < 0.25) due to adsorption and cluster formation at the hydrophilic metal sites of the compound. The steep rise at 0.25 < P/P_0 < 0.45 has been soundly explained with the consecutive filling of first the 25 Å, and then the 29 Å pores. The low water adsorption of MIL-100(Al) (0.5 $g_{water}/g_{adsorbent}$) was explained by the incomplete H_2O filling of the pores. Additionally, the presence of hydrophobic sites, e.g. small amounts of unremoved H_3btc may inhibit complete wetting of the pore walls.[32] Hydrothermal cycle stability of MIL-100(Al) was quantified with samples exposed to a humidified gas flow (Fig.10). This material was relatively water-stable with small sub-sequential losses of water capacities and porosities, and no detectable loss of crystallinity (XRD).

Preprints (www.preprints.org) | NOT PEER-REVIEWED | Posted: 13 July 2018 doi:10.20944/preprints201807.0242.v1

Peer-reviewed version available at Nanomaterials 2018, 8, 661; doi:10.3390/nano8090661

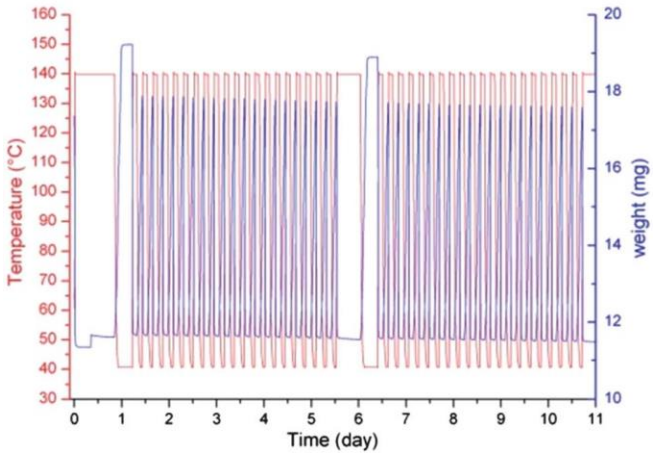

Figure 10. Temperature profile and load signal of the MIL-100(Al) cycling experiment, acquired at p_{H2O}= 5.6 kPa. (Reproduced with permission from ref. [32])

Iron (Fe) based MOFs

Another porous MOF, MIL-100(Fe) consists of iron (III) tricarboxylates. The cages are formed by supertetrahedra, which are constructed of iron trimers linked by the tricarboxylate linkers. The pore diameter of the supertetrahedra is slightly smaller than in MIL-101(Cr) with 6.6 Å in diameter.[69] Nitrogen physisorption measurements revealed a Langmuir surface area larger than 2800 m^2/g. MIL-100(Fe) has a polymodal pore size distribution and has both micropores and mesopores. The presence of mesopores leads to water adsorption in a higher-pressure region than typically observed for microporous materials with a more or less polar inner surface such as HKUST-1. The steep adsorption step at P/P_0 = 0.3 - 0.4 indicates the filling of the mesoporous cages. Similar to HKUST-1, adsorption on the available metal sites occurs at first. The filling of the mesopores then occurs consecutively, first by filling the smaller 25 Å pores followed by filling of the 29 Å pores. The saturation is obtained at P/P_0 = 0.5 and there is only a slight additional increase of the adsorbed water volume which is due to the adsorption of molecules in the inter-particulate voids of the material. The water adsorption capacity of as-synthesized MIL-100(Fe) can reach as high as 0.75 $g_{water}/g_{adsorbent}$ at 298 K.[70] The desorption branch of MIL-100 (Fe) obtained a distinct hysteresis especially, for the large mesopores. This phenomenon is widely known for mesoporous materials, yet undesired for the intended application, as it considerably decreases the usable part of the loading. Since MIL-100(Fe) is synthesized in water, it should have a high water stability. Additionally, this MOF is based on iron, which is much more suitable for industrial use than copper, chromium or cobalt based MOFs regarding toxicity.

4. Modification/functionalization of MOFs based on water adsorption

One of the advantages of MOF materials compared with other conventional porous materials adsorbent is not only the tunable nature with the choice of metal ions and the linker species but also the modification or functionalization ability to tune their properties.

Preprints (www.preprints.org) | NOT PEER-REVIEWED | Posted: 13 July 2018 doi:10.20944/preprints201807.0242.v1

Peer-reviewed version available at Nanomaterials 2018, 8, 661; doi:10.3390/nano8090661

Functionalized MOFs bearing ligand functional group

The water uptake capacity of MOFs is not only determined by the available porosity, but also by the hydrophobicity/hydrophilicity of the ligand, with the hydrogen-bonding capabilities of functional groups and a possible structural transition of the adsorbent material.[42, 43, 71] In order to tune the water uptake to lower P/P_0 values, the organic linker can be modified with a hydrophilic functional group. Several functional groups in the ligand molecules such as nitro-terephthalate (-NO_2), amino-terephthalate (-NH_2), and sulfo-terephthalate (-SO_3H), etc. were investigated for the water adsorption behavior comparable to the non-functionalized ligand containing MOFs. The MIL-101 and MIL-101 derivatives were used to elucidate the effect of ligand functional groups for water adsorption.[35] Different isotherm lines were found among the water adsorption of MIL-101, MIL-101-NO_2, MIL-101-NH_2, and MIL-101-SO_3H. It is worth noting that the isotherm lines of MIL-101-NH_2 and MIL-101-SO_3H shifted to lower P/P_0 values compared with that of MIL-101, which was attributed to the highly hydrophilic groups on their pore surfaces. In contrast, the isotherm of MIL-101-NO_2 shows almost the same profile as that of MIL-101 in terms of water uptake pressure, which might be because of the lower hydrophilicity of the NO_2 group. The introduction of a hydrophilic group such as -NH_2 or -SO_3H could provide a hydrophilic environment inside the pore, resulting in a stronger interaction between the pores and water molecules. As a result, MIL-101-SO_3H and MIL-101-NH_2 start to adsorb water in a lower pressure region than that for the original MIL-101. Similar results were obtained for the study of 2-amino benzene dicarboxylic acid (NH_2-BDC) bridging as linkers of cyclic octamer corners or edge sharing $TiO_5(OH)$ octahedrons generating $Ti_8O_8(OH)_4$-$(O_2CC_6H_5$-CO_2-$NH_2)_6$ or NH_2-MIL-125. Kim et al. demonstrated that water adsorption on NH_2-MIL-125 showed a sharp rise of adsorption at a relative pressure of about (P/P_0) 0.2 making this MOF a promising new candidate for adsorptive air conditioning driven by a low-grade heat.[72] The study indicates that the carboxylate and the O-Ti-O groups are primary adsorption centers forming hydrogen bonds with water molecules. However, the highly hydrophilic -NH_2 groups could be another type of primary adsorption center. To verify the hydrothermal stability of NH_2-MIL-125, the material was subjected to multiple adsorptions/desorption cycles applying conditions such as P = 2.36 kPa, T_{ads} = 313 K, and T_{des} = 383 K. The experiment revealed that the water uptake displayed a small decrease during the first cycle (from 0.42 to 0.40 g/g), thereafter the uptake turn out to be stable (w = 0.39 g/g) across the remaining cycles. The texture characteristics of the studied MIL after 10 cycles (NH_2-MIL-125-10AC) changed only slightly with the specific surface area S_{sp} dropping from 1300 to 1230 m^2/g and the pore volume V_P declined from 0.56 to 0.54 cm^3/g.

The effect of halogen ions (F, Cl) and sulphate (SO_4) incorporated in the MOF structure influencing the water adsorption was investigated using MIL-100(Cr).[31] The free counter anion in the MOF pores was replaced with other counter anion using different inorganic acids (F = hydrofluoric acid, Cl = hydrochloric acid, and SO_4 = sulfuric acid). An exceptionally large amount of water was adsorbed on MIL-100-F (> 0.65 $g_{water}/g_{adsorbent}$) over the non-ionic functional MOF (0.5 $g_{water}/g_{adsorbent}$) and the adsorption amount remains stable even after two thousand adsorption/desorption cycles. Interesting, the counter anion affects the water uptake, it was observed that the values of P/P_0 for the steps are different. The steps in the isotherm of MIL-100-SO_4 moved to lower P/P_0 values compared with those of the other compounds. In the meantime,

the isosteric heats of adsorption (q_{st}) on MIL-100-SO_4 showed the largest values and MIL-100-Cl demonstrated the smallest values, a tendency similar to the hydration energies. According to the hydration energy and isosteric heat of adsorption, the interaction between water and sulfate anion is stronger than that between water and chloride anion. As a result, the adsorption for MIL-100-SO_4 begins at a lower pressure than for MIL-100-Cl. Monte Carlo simulations in a grand canonical ensemble (GCMC) were carried out to confirm the influence of the three anions in the MIL-100(Fe) structures (e.g., F−, Cl−, or OH−) for water adsorption isotherms.[73] In the simulations, the water adsorption behavior and the relative structural stability of MIL-100(Fe) were investigated. The small cages, which provide a stronger interaction with water molecules compared to the large cages, were completely filled with water at a notably lower pressure. Among the three structures, because of the strongest interaction between the terminal F^- anion and water molecules, the adsorption isotherm of MIL-100(Fe)−F displays the highest adsorption capability with the occurrence of water condensation at a much smaller relative pressure. It can be concluded that the counter anions incorporated in the structure tune the guest uptake, although adsorption properties of MOFs are usually changed by the pore size or organic ligands of the frameworks.

A series of isostructural UiO-66(Zr) with different functional groups such as -NH_2, -OH, and -$(OH)_2$ were employed to functionalize the BDC linker to investigate the hydrophilic effect of the groups.[74] All the functionalized UiO-66(Zr) materials showed enhanced water adsorption in the low P/P_0 relative pressure due to the augmented interactions with water molecules, leading to isotherms that approached the *type I* shape (Fig.11a). However, water adsorption of the functionalized UiO-66(Zr) materials in the high P/P_0 decreased significantly compared with the original UiO-66(Zr) as a consequence of the decreased surface area due to the insertion of bulky groups in the pores. The hysteresis in water adsorption and desorption isotherms, especially at low relative humidity conditions may be elucidated by rehydroxylation of Zr-clusters during the water adsorption.[42, 75] On the other hand, the unsaturated metal sites influenced the water adsorption/desorption and a study on the metal series of isostructural MIL-100(M) materials (M = Cr, Fe, and Al) was performed. As displayed in Fig. 11b, the water adsorption isotherms of MIL-100(Cr), MIL-100(Fe), and MIL-100(Al) almost coincided with one another. The isotherm types were similar to *type IV*, but two steps at which the water loadings noticeably increased were clearly observed at P/P_0 = 0.25 and 0.4 for all three MOFs. These two steps revealed that capillary condensations occur step by step in two types of pores. The water uptake of the three MIL-100(M) materials at P/P_0 = 0.8 was approximately 820–900 cm^3/g, which is approximately 45–50% compared with MIL-101(Cr). The water uptakes of MIL-101(Cr) and MIL-100(M) at P/P_0 = 0.8 correlated well with the BET surface areas. These results indicate that the type of unsaturated metal in MIL-100(M) does not significantly affects the water adsorption. Nonetheless, some interesting cyclic water adsorption/desorption behaviors depend on the type of unsaturated metal.

Preprints (www.preprints.org) | NOT PEER-REVIEWED | Posted: 13 July 2018 doi:10.20944/preprints201807.0242.v1

Peer-reviewed version available at Nanomaterials 2018, 8, 661; doi:10.3390/nano8090661

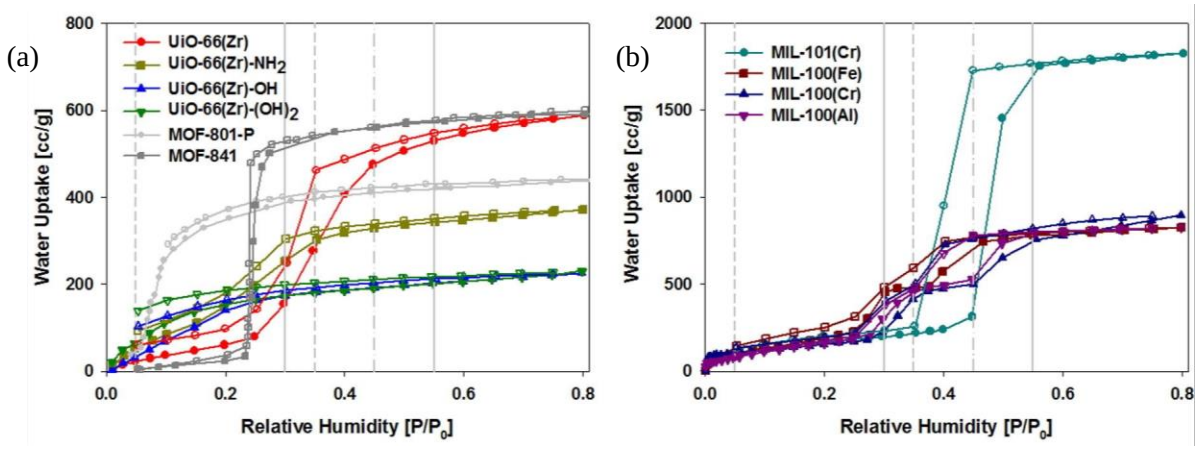

Figure 11. Water adsorption/desorption isotherms of the series of MOFs at 298 K. (Reproduced with permission from ref.[74])

Functionalized MOFs with composite materials

Composite adsorbents are studied and developed with mainly two goals: 1) to improve the heat and mass transfer performance of chemical adsorbents, especially via the swelling, and 2) to increase the adsorption quantity of physical adsorbents via agglomeration phenomena. The composite adsorbents made from porous materials and chemical sorbents are commonly a combination.

Encapsulation of inorganic compounds in porous materials was explored to enhance the water uptake. The porous materials act as a media to disperse the salt particles and can provide good heat and mass transport for these salt particles. To date, different porous materials have been explored for encapsulation, including silica, filosilicates, activated carbon, and microporous zeolites.[76-78] Recently, the spherical hollow superstructure/beads of UiO-66 and UiO-66-NH_2 encapsulated with inorganic salts were developed via spray drying. The inorganic salts $CaCl_2$ and LiCl were selected for encapsulation during the assembly of the nanosized crystals.[79] The water sorption isotherm of $CaCl_2$@UiO-66 at 298 K showed two segments with a steep increase in the water uptake (Fig. 12). These two steps were attributed to the formation of $CaCl_2 \cdot 0.33H_2O$ at a relative humidity (RH) of 3% (water uptake of 0.15 $g_{water}/g_{adsorbent}$) and to the further transformation of this hydrate to $CaCl_2 \cdot 2H_2O$ at RHs ranging from 10% to 16% (water uptake of 0.33 $g_{water}/g_{adsorbent}$). Thereafter, the sorption curve ascended monotonically, indicating the formation of an aqueous solution of the salt and reaching a maximum water uptake of 1.93 $g_{water}/g_{adsorbent}$ at an RH of 90%.[80, 81] Interestingly, a hysteresis loop at low pressures (P/P_0 = 0.10–0.16) was observed in the desorption branch due to the structural changes in the transition from $CaCl_2 \cdot 2H_2O$ hydrate to $CaCl_2 \cdot 0.33H_2O$ hydration. A hypothetical mechanism for the water sorption was suggested and the following steps take place: the anhydrous $CaCl_2$ particles confined in the micropores of UiO-66 and/or in the interparticular voids of the superstructures adsorb water and transform into crystalline $CaCl_2 \cdot 0.33H_2O$. Then, this hydrate adsorbs more water and is converted to crystalline $CaCl_2 \cdot 2H_2O$ and finally, the salt is completely dissolved

Preprints (www.preprints.org) | NOT PEER-REVIEWED | Posted: 13 July 2018 doi:10.20944/preprints201807.0242.v1

Peer-reviewed version available at Nanomaterials 2018, 8, 661; doi:10.3390/nano8090661

filling the pores and/or voids. Remarkably, the maximum uptake at 90% RH (1.93 $g_{water}/g_{adsorbent}$) remained constant with the number of cycles, confirming the stability of this composite to water sorption/desorption processes (Fig. 2c). On the other hand, $CaCl_2$@UiO-66-NH_2_38 showed a maximum uptake of 1.76 $g_{water}/g_{adsorbent}$, which is lower compared with its analogue based on UiO-66, but it retained 0.12 $g_{water}/g_{adsorbent}$ (6.8% of the total uptake) of water at an RH of 0%, which is a double amount than that of its UiO-66 analogue.

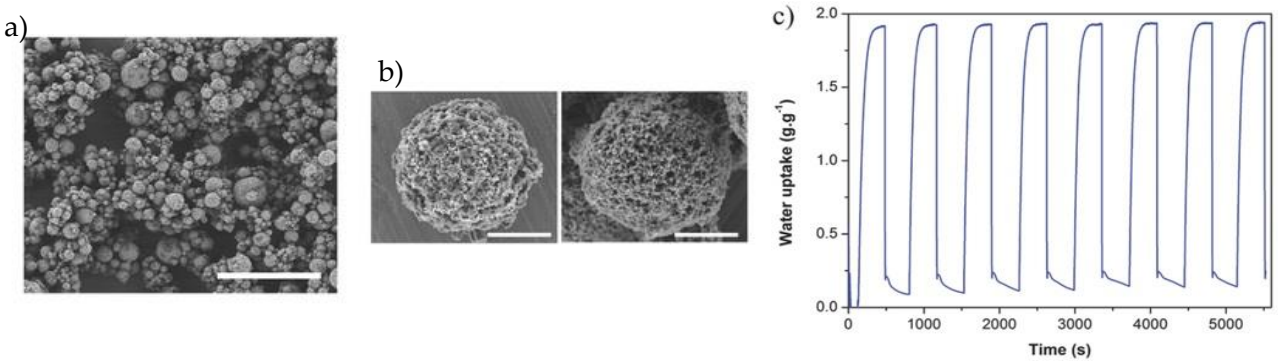

Figure 12. a) Representative FESEM image of microspherical $CaCl_2$@UiO-66, b) FESEM images of microspherical $CaCl_2$@UiO-66_38 superstructures before (left) and after (right) incubation in ethanol, c) adsorption and desorption cycles for $CaCl_2$@UiO-66_38. Scale bars: a) 20 μm, b) 3 μm. [Reproduced with permission from ref.[79]]

Another route to improve the adsorption performance of MOFs can be realized via increasing the atomic density of the adsorbent material. For example, MOFs combined with dense carbon substrates e.g. graphene oxide (GO) can produce composites (MOF@GO) with excellent adsorption performances such as MOF-5@GO [82], MIL-101(Cr)@GO [83], Cu-BTC@GO [84]. It was reported that the incorporation of GO into MOFs structures would noticeably improve the adsorption performances of the composites for adsorption of CO_2, H_2O, and VOCs. A series of composites Cu-BTC@GO with various GO loading were synthesized at room temperature.[85] The Cu-BTC@GO composite demonstrated a superhigh adsorption capacity for ethanol up to 13.60 mmol/g at 30°C, which was attributed to the introduction of GO leading to an increase in the surface dispersive forces and the mesoporous volume of Cu-BTC@GO. The ethanol adsorption capacity was higher than many other MOFs including Cu-BTC, MIL-101, MIL-53, and so on under similar conditions. The MOF composite exceptional adsorption properties paid the price via extremely low thermal conductivity due to their large pore sizes and high free volumes. The low thermal conductivity limits the ability of the heat transfer processes to reach the desired operating temperatures quickly during both the adsorption and desorption phases. The thermal properties in addition to the hydrophilicity (as the oxygen in GO strongly binds to water molecules through hydrogen bonding interactions) of the GO was the motivation to investigate the characteristics of MIL-101(Cr)/GO composites for the water adsorption and the thermal conductivity.[86] Two synthesized composites (with 2 wt% GO and 5 wt% GO) showed an increased uptake in the high relative pressure range, which is consistent with the suggestion that the oxygen functionalities of GO (hydroxyl, carboxyl, and epoxy) were able to coordinate to the

Preprints (www.preprints.org) | NOT PEER-REVIEWED | Posted: 13 July 2018 doi:10.20944/preprints201807.0242.v1

Peer-reviewed version available at Nanomaterials 2018, 8, 661; doi:10.3390/nano8090661

metallic centers of the MIL-101(Cr) structure and hence new pores were created at the interface of the structure and the graphene layers. The 2 wt% GO composite showed a maximum water uptake of 1.56 $g_{water}/g_{adsorbent}$ while the 5 wt% GO composite reached a value of 1.47 $g_{water}/g_{adsorbent}$. The small reduction in water adsorption for the 5 wt% GO composite may be attributed to the fact that GO is a non-porous material and may cause pore blocking, and hence, lower the accessible surface area and pore volume of the composites if more GO is incorporated into MIL-101(Cr) (Fig.13). Based on the equilibrium data, the water loading difference, which is the difference between the amount of water adsorbed in the adsorption process and the amount of water remaining in the pores after the desorption process, is 1.36 $g_{water}/g_{adsorbent}$ for the parent material while amounts to 1.33 $g_{water}/g_{adsorbent}$ for the composite. Those values are much higher than those reported for other types of MOFs under similar operating conditions. Aluminum fumarate can have a water loading difference of 0.45 $g_{water}/g_{adsorbent}$[46] while MIL-100(Al) reaches a value of 0.4 $g/g_{adsorbent}$ and MIL-100(Fe) reaches 0.65 $g/g_{adsorbent}$.[32] Furthermore, a good thermal conductivity is crucial in adsorption and desorption processes. Figure 13 shows the thermal conductivity of the material as a function of temperature. It can be seen that the thermal conductivity of neat MIL-101(Cr) is 0.05 W $(m\ K)^{-1}$ at 303 K and increases linearly to reach 0.103 W $(m\ K)^{-1}$ at 473 K. The effect of the presence of graphene oxide at different ratios was also investigated. Despite the presence of the oxygen atoms, which typically enhances phonon scattering, the enhancement of the thermal conductivity observed could be attributed to the increase in the interlayer coupling due to interactions between the oxygen atom of the GO and the MIL-101(Cr) framework.[87]

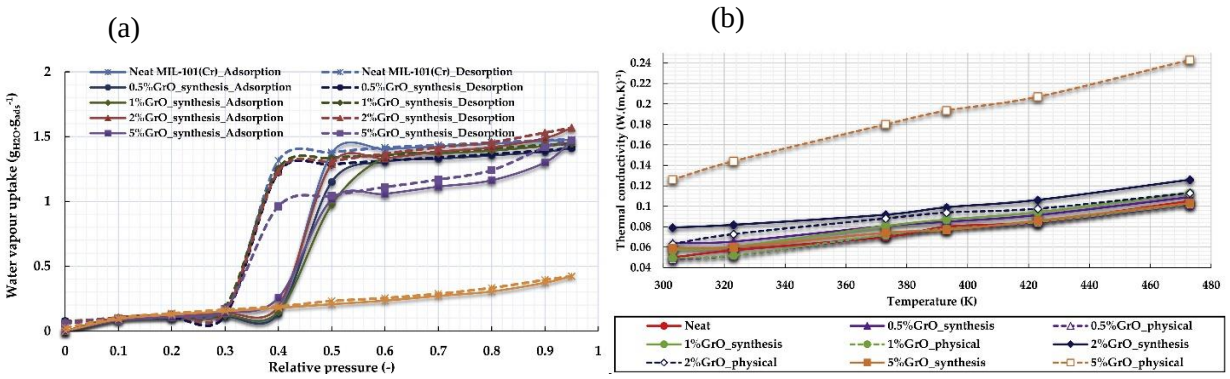

Figure 13. a) Water adsorption isotherms and b) Thermal conductivity of MIL-101(Cr) and MIL/GO composites. [Reproduced with permission from ref.[86]]

Since MOFs may have quite high surface areas, this issue deserves attention. Another advantage of these materials is the relatively low temperatures required for desorbing their water contents. However, it is also crucial to check carefully their hydrothermal stabilities due to the observations that some of these materials are not stable in the presence of water and/or at relatively high temperatures, resulting in dramatic decreases in the adsorption capacities. Hydrothermal stability of MOFs can also be improved by shielding the metal-linker bond from water vapor using sterically demanding and hydrophobic linkers. However, as in many cases, an aqua ligand or a free coordination site on the metal atom serves as an anchor for water cluster

formation, hydrophilicity is usually strongly reduced in such cases, and the MOF may not adsorb any water at all.[29] For example, zinc imidazolate ZIF-8 is hydrothermally stable because no water is adsorbed.[88, 89] A zinc-based MOFs showed increased hydrothermal stability when water adsorption is prevented due to interpenetration or pore blocking.[90] For use in adsorption heat transformation, hydrothermal stability cannot be deduced merely by retrieving the MOF from an aqueous suspension without structural damage but needs to be verified through a larger number of water vapor adsorption/desorption cycles. It still seems to be a challenge to find materials which have relatively high water uptake in a narrow relative humidity range while maintaining high structural integrity. The attempts to increase the water stability of MOFs have led to declines in their water uptake capacity due to enhanced hydrophobicity and reduction in surface areas.

Outlook

Metal-Organic Frameworks (MOFs) are new porous materials having a high surface area, pore size and volume of which the geometry and properties can be tuned for the required application. Moreover, a high capability of solid-gas adsorption is a conversional criterion for a high potential as an adsorbent for heat transformation applications. However, it is not a general rule that a strong "adsorbed-adsorbent" interaction is obviously favorable to obtain a high adsorption capacity of the adsorbed vapor (working fluid) since a strong interaction requires a too high desorption temperature (>200-300°C) which might not be provided from common heat sources (solar radiation, engine wastes, etc.). Thus, the high adsorption capacity caused by a strong adsorption interaction becomes, quite contrary, unfavorable for the transformation of low-temperature heat. On the other hand, a too weak "adsorbed-adsorbent" interaction is auspicious for desorption, however, does not allow during the adsorption phase sufficient driving force for adsorbed "sucking" and, hence, for the cold generation. Thus, an optimal adsorbent should provide a moderate affinity toward adsorbed molecules that depends on particular boundary conditions of the cycle.

MOFs normally occur after synthesis as a fine powder and they are not applicable in most industrial processes, nor for heat transformation. The integration of MOFs as adsorbent and heat exchanger are new efficient applications and can be applied at real operating conditions of heat transformation technologies. Considering the thermodynamics, the former configuration (Heat transformation systems) is very simple and ensures a good vapor transport but is considered to suffer from a poor heat transfer due to the high thermal resistance between the adsorbent grains. As a result, adsorption kinetics is expected to be slow and limited by the heat transfer. Coated MOF adsorbent material, in which the MOFs are directly connected to the surface (fins tube exchanger) or with a binder (ex situ) could directly solve the former issue. Elimination of the limitations originating from inefficient heat transfer inside the adsorber as well as the easy manipulation of the adsorbent thickness, in a manner avoiding mass transfer limitations, may be achieved by using coatings. Significant improvements have been demonstrated to take place in these systems when the adsorbent is directly crystallized on metal heat exchanger surfaces as coatings, instead of being used in powder or pellet form.[91] The approach in which a binder is applied to produce a coating is based on a procedure developed previously for zeolites and direct crystallization via a thermal gradient method. The in situ coatings are now the most popular

method for the heat transformation applications.[92-94] As mentioned before MOF-coatings can generally be produced via two routes: Binder-based coatings and direct crystallization. Still, several key factors in the design and manufacturing such as layer thickness and the binder type influence the heat transfer coefficient, the mechanical stability of such coatings, the coating texture, etc. and need further improvement.

Macrocellular foam composite adsorbent material is a new approach for an innovative adsorber, and is not necessarily an alternative to the adsorbent coating process.[95, 96] The principle is based on the use of composite adsorbent filled silicone foams that can improve the adsorption surface area without altering the adsorption pump dynamic performances. Practical problems arising from adsorbent is that the high thickness bed enhanced the mass transfer and thermal conductivity. A directly coated adsorbent on the heat exchanger wall (Fins) displays a limited heat transfer between the heat exchanger surface and the adsorbent, the mass transfer resistance is substantially reduced due to the very thin adsorbent layer.[93, 97] However, multiple depositions are necessary in order to reach an acceptable adsorbent layer thickness (< 0.1 mm). Moreover, in this approach, the adsorbent material can be homogeneously distributed along the surface of macrocellular foam generating a product with significant advantages in terms of the cheapness of the synthesis process, low weight and large adsorbent thickness, high vapor diffusion permeability and good hydrothermal and mechanical stability. The zeolite-embedded silicon foam evidenced the effective sorption and desorption processes, giving to composite adsorbents materials with silicon foam greater advantages than other zeolite containing systems (e.g. coating, picking, direct growth etc.) for heat pump applications. [96]

5. Conclusion

The adsorbent material is a key factor in the design and manufacturing of this application. In principle, a huge amount of MOFs have already been synthesized, but only for a few of them, the adsorption heat transformation has been studied. We believe that future screening of MOFs as adsorbent materials for heat transformation applications will reveal novel and highly efficient working adsorbents. The development of novel adsorbents is needed in order to propel adsorption based water adsorption from scientific curiosities into real-life applications. Next generation adsorbents should have: (i) a high chemical stability to water, (ii) a tailorable hydrophilicity, and (iii) an adjustable pore diameter to fine-tune the adsorption profile and modulate the sorption kinetics. However, consideration to develop this technology is until now more focused on the decrease of unit costs and the increase in energy efficiency. Adsorption is focused in finding more efficient working pairs, and for the storage, the first prototypes are tested and new ones are designed with different or enhanced storage materials and new reactor concepts to optimize the energy output. All in all, we hope that this review will give new impulses to target-oriented research on novel adsorbents based on MOFs and their derivative modifications which may be beneficial for further heat transformation applications.

Acknowledgment

The authors gratefully acknowledge ‘‘State Key Lab of Advanced Technology for Materials Synthesis and Processing” for financial support. F.V., S.C., and M.S.Y. acknowledge the support from the Russian Foundation for Basic Research (N° 18-29-04047) and Tomsk Polytechnic

University Competitiveness Enhancement Program grant (VIU-195/2018). S.C. acknowledges the support of the National Natural Science Foundation of China (No.21502146).

References

1. Isaac, M.; Van Vuuren, D.P. Modeling global residential sector energy demand for heating and air conditioning in the context of climate change. Energy policy **2009**, 37, 507-521.
2. Alefeld, G.; Radermacher, R., Heat conversion systems, CRC press, 1993.
3. Schmidt, F.;Henninger, S.;Stach, H.;Jänchen, J.; Henning, H., Novel adsorbents for solar cooling applications, in: International Conference Solar Air Conditioning, Kloster Banz, Bad Staffelstein, Germany, 2005, pp. 39-44.
4. Henning, H.-M. Solar assisted air conditioning of buildings–an overview. Appl. Therm. Eng. **2007**, 27, 1734-1749.
5. Demir, H.;Mobedi, M.; Ülkü, S. A review on adsorption heat pump: Problems and solutions. Renewable Sustainable Energy Rev. **2008**, 12, 2381-2403.
6. Ng, K.;Chua, H.;Chung, C.;Loke, C.;Kashiwagi, T.;Akisawa, A.; Saha, B. Experimental investigation of the silica gel–water adsorption isotherm characteristics. Appl. Therm. Eng. **2001**, 21, 1631-1642.
7. James, S.L. Metal-organic frameworks. Chem. Soc. Rev. **2003**, 32, 276-288.
8. Chaemchuen, S.;Kabir, N.A.;Zhou, K.; Verpoort, F. Metal–organic frameworks for upgrading biogas via CO 2 adsorption to biogas green energy. Chem. Soc. Rev. **2013**, 42, 9304-9332.
9. Chughtai, A.H.;Ahmad, N.;Younus, H.A.;Laypkov, A.; Verpoort, F. Metal–organic frameworks: versatile heterogeneous catalysts for efficient catalytic organic transformations. Chem. Soc. Rev. **2015**, 44, 6804-6849.
10. Henninger, S.K.;Jeremias, F.;Kummer, H.; Janiak, C. MOFs for use in adsorption heat pump processes. Eur. J. Inorg. Chem. **2012**, 2012, 2625-2634.
11. Younos, T.; Tulou, K.E. Overview of desalination techniques. J. Contemp. Phys. **2005**, 132, 3-10.
12. Youssef, P.G.;Dakkama, H.;Mahmoud, S.M.; AL-Dadah, R.K. Experimental investigation of adsorption water desalination/cooling system using CPO-27Ni MOF. Desalination **2017**, 404, 192-199.
13. Wang, X.; Ng, K.C. Experimental investigation of an adsorption desalination plant using low-temperature waste heat. Appl. Therm. Eng. **2005**, 25, 2780-2789.
14. Ng, K.C.;Xiao-Lin, W.;Gao, L.;Chakraborty, A.;Saha, B.B.;Koyama, S.;Akisawa, A.; Kashiwagi, T., Apparatus and method for desalination, in, Google Patents, 2013.
15. Thu, K.;Ng, K.C.;Saha, B.B.;Chakraborty, A.; Koyama, S. Operational strategy of adsorption desalination systems. Int. J. Heat Mass Transfer **2009**, 52, 1811-1816.
16. Henninger, S.;Schmidt, F.; Henning, H.-M. Water adsorption characteristics of novel materials for heat transformation applications. Appl. Therm. Eng. **2010**, 30, 1692-1702.
17. Brancato, V.; Frazzica, A. Characterisation and comparative analysis of zeotype water adsorbents for heat transformation applications. Sol. Energy Mater. Sol. Cells **2018**, 180, 91-102.

18. You, W.;Liu, Y.;Howe, J.D.; Sholl, D.S. Competitive Binding of Ethylene, Water, and Carbon Monoxide in Metal–Organic Framework Materials with Open Cu Sites. J. Phys. Chem. C **2018**, 122, 8960-8966.
19. Tatlier, M.;Munz, G.; Henninger, S.K. Relation of water adsorption capacities of zeolites with their structural properties. Microporous Mesoporous Mater. **2018**.
20. Aristov, Y.I. Novel materials for adsorptive heat pumping and storage: screening and nanotailoring of sorption properties. J. Chem. Eng. Jpn. **2007**, 40, 1242-1251.
21. Canivet, J.;Bonnefoy, J.;Daniel, C.;Legrand, A.;Coasne, B.; Farrusseng, D. Structure–property relationships of water adsorption in metal–organic frameworks. New J. Chem. **2014**, 38, 3102-3111.
22. Burtch, N.C.;Jasuja, H.; Walton, K.S. Water stability and adsorption in metal–organic frameworks. Chem. Rev. **2014**, 114, 10575-10612.
23. Chaemchuen, S.;Wang, J.C.;Gilani, A.G.; Francis, F.V. METAL-ORGANIC FRAMEWORKS APPLIED FOR WATER PURIFICATION. Resource Efficient Technologies **2018**, 1, 1-16.
24. Taylor, J.M.;Vaidhyanathan, R.;Iremonger, S.S.; Shimizu, G.K. Enhancing water stability of metal–organic frameworks via phosphonate monoester linkers. J. Am. Chem. Soc. **2012**, 134, 14338-14340.
25. Canivet, J.;Fateeva, A.;Guo, Y.;Coasne, B.; Farrusseng, D. Water adsorption in MOFs: fundamentals and applications. Chem. Soc. Rev. **2014**, 43, 5594-5617.
26. Jasuja, H.;Burtch, N.C.;Huang, Y.-g.;Cai, Y.; Walton, K.S. Kinetic water stability of an isostructural family of zinc-based pillared metal–organic frameworks. Langmuir **2013**, 29, 633-642.
27. Reinsch, H.;van der Veen, M.A.;Gil, B.;Marszalek, B.;Verbiest, T.;De Vos, D.; Stock, N. Structures, sorption characteristics, and nonlinear optical properties of a new series of highly stable aluminum MOFs. Chemistry of Materials **2012**, 25, 17-26.
28. Reinsch, H.;Marszalek, B.;Wack, J.;Senker, J.;Gil, B.; Stock, N. A new Al-MOF based on a unique column-shaped inorganic building unit exhibiting strongly hydrophilic sorption behaviour. Chemical Communications **2012**, 48, 9486-9488.
29. Küsgens, P.;Rose, M.;Senkovska, I.;Fröde, H.;Henschel, A.;Siegle, S.; Kaskel, S. Characterization of metal-organic frameworks by water adsorption. Microporous Mesoporous Mater. **2009**, 120, 325-330.
30. Furukawa, H.;Gándara, F.;Zhang, Y.-B.;Jiang, J.;Queen, W.L.;Hudson, M.R.; Yaghi, O.M. Water Adsorption in Porous Metal–Organic Frameworks and Related Materials. Journal of the American Chemical Society **2014**, 136, 4369-4381.
31. Akiyama, G.;Matsuda, R.; Kitagawa, S. Highly porous and stable coordination polymers as water sorption materials. Chem. Lett. **2010**, 39, 360-361.
32. Jeremias, F.;Khutia, A.;Henninger, S.K.; Janiak, C. MIL-100(Al, Fe) as water adsorbents for heat transformation purposes-a promising application. J. Mater. Chem. **2012**, 22, 10148-10151.
33. Wickenheisser, M.;Jeremias, F.;Henninger, S.K.; Janiak, C. Grafting of hydrophilic ethylene glycols or ethylenediamine on coordinatively unsaturated metal sites in MIL-100(Cr) for improved water adsorption characteristics. Inorganica Chimica Acta **2013**, 407, 145-152.

34. Ehrenmann, J.;Henninger, S.K.; Janiak, C. Water Adsorption Characteristics of MIL-101 for Heat-Transformation Applications of MOFs. Eur. J. Inorg. Chem. **2011**, 2011, 471-474.
35. Akiyama, G.;Matsuda, R.;Sato, H.;Hori, A.;Takata, M.; Kitagawa, S. Effect of functional groups in MIL-101 on water sorption behavior. Microporous Mesoporous Mater. **2012**, 157, 89-93.
36. Khutia, A.;Rammelberg, H.U.;Schmidt, T.;Henninger, S.; Janiak, C. Water Sorption Cycle Measurements on Functionalized MIL-101Cr for Heat Transformation Application. Chemistry of Materials **2013**, 25, 790-798.
37. Canivet, J.;Bonnefoy, J.;Daniel, C.;Legrand, A.;Coasne, B.; Farrusseng, D. Structure-property relationships of water adsorption in metal-organic frameworks. New Journal of Chemistry **2014**, 38, 3102-3111.
38. Jeremias, F.;Lozan, V.;Henninger, S.K.; Janiak, C. Programming MOFs for water sorption: amino-functionalized MIL-125 and UiO-66 for heat transformation and heat storage applications. Dalton Trans. **2013**, 42, 15967-15973.
39. Shigematsu, A.;Yamada, T.; Kitagawa, H. Wide control of proton conductivity in porous coordination polymers. Journal of the American Chemical Society **2011**, 133, 2034-2036.
40. Wade, C.R.;Corrales-Sanchez, T.;Narayan, T.C.; Dincă, M. Postsynthetic tuning of hydrophilicity in pyrazolate MOFs to modulate water adsorption properties. Energy & Environmental Science **2013**, 6, 2172-2177.
41. Liu, J.;Wang, Y.;Benin, A.I.;Jakubczak, P.;Willis, R.R.; LeVan, M.D. CO2/H2O Adsorption Equilibrium and Rates on Metal−Organic Frameworks: HKUST-1 and Ni/DOBDC. Langmuir **2010**, 26, 14301-14307.
42. Schoenecker, P.M.;Carson, C.G.;Jasuja, H.;Flemming, C.J.; Walton, K.S. Effect of water adsorption on retention of structure and surface area of metal–organic frameworks. Ind. Eng. Chem. Res. **2012**, 51, 6513-6519.
43. Cmarik, G.E.;Kim, M.;Cohen, S.M.; Walton, K.S. Tuning the Adsorption Properties of UiO-66 via Ligand Functionalization. Langmuir **2012**, 28, 15606-15613.
44. Henninger, S.K.;Habib, H.A.; Janiak, C. MOFs as adsorbents for low temperature heating and cooling applications. J. Am. Chem. Soc. **2009**, 131, 2776-2777.
45. Saha, B.B.;El-Sharkawy, I.I.;Miyazaki, T.;Koyama, S.;Henninger, S.K.;Herbst, A.; Janiak, C. Ethanol adsorption onto metal organic framework: Theory and experiments. Energy **2015**, 79, 363-370.
46. Jeremias, F.;Frohlich, D.;Janiak, C.; Henninger, S.K. Advancement of sorption-based heat transformation by a metal coating of highly-stable, hydrophilic aluminium fumarate MOF. RSC Adv. **2014**, 4, 24073-24082.
47. Gordeeva, L.G.;Solovyeva, M.V.; Aristov, Y.I. NH2-MIL-125 as a promising material for adsorptive heat transformation and storage. Energy **2016**, 100, 18-24.
48. Chui, S.S.-Y.;Lo, S.M.-F.;Charmant, J.P.;Orpen, A.G.; Williams, I.D. A chemically functionalizable nanoporous material [Cu3 (TMA) 2 (H2O) 3] n. Science **1999**, 283, 1148-1150.
49. Rowsell, J.L.; Yaghi, O.M. Effects of functionalization, catenation, and variation of the metal oxide and organic linking units on the low-pressure hydrogen adsorption properties of metal− organic frameworks. J. Am. Chem. Soc. **2006**, 128, 1304-1315.

50. Schlichte, K.;Kratzke, T.; Kaskel, S. Improved synthesis, thermal stability and catalytic properties of the metal-organic framework compound Cu3 (BTC) 2. Microporous Mesoporous Mater. **2004**, 73, 81-88.
51. Prestipino, C.;Regli, L.;Vitillo, J.;Bonino, F.;Damin, A.;Lamberti, C.;Zecchina, A.;Solari, P.;Kongshaug, K.; Bordiga, S. Local structure of framework Cu (II) in HKUST-1 metallorganic framework: spectroscopic characterization upon activation and interaction with adsorbates. Chem. Mater. **2006**, 18, 1337-1346.
52. Kitaura, R.;Fujimoto, K.;Noro, S.i.;Kondo, M.; Kitagawa, S. A Pillared-Layer Coordination Polymer Network Displaying Hysteretic Sorption:[Cu2 (pzdc) 2 (dpyg)] n (pzdc= Pyrazine-2, 3-dicarboxylate; dpyg= 1, 2-Di (4-pyridyl) glycol). Angew. Chem. Int. Ed. **2002**, 114, 141-143.
53. Férey, G.;Mellot-Draznieks, C.;Serre, C.;Millange, F.;Dutour, J.;Surblé, S.; Margiolaki, I. A chromium terephthalate-based solid with unusually large pore volumes and surface area. Science **2005**, 309, 2040-2042.
54. Baerlocher, C.;McCusker, L.B.; Olson, D.H., Atlas of zeolite framework types, Elsevier, 2007.
55. Llewellyn, P.L.;Bourrelly, S.;Serre, C.;Vimont, A.;Daturi, M.;Hamon, L.;De Weireld, G.;Chang, J.-S.;Hong, D.-Y.;Kyu Hwang, Y.;Hwa Jhung, S.; Férey, G. High Uptakes of CO2 and CH4 in Mesoporous Metal—Organic Frameworks MIL-100 and MIL-101. Langmuir **2008**, 24, 7245-7250.
56. Chowdhury, P.;Bikkina, C.; Gumma, S. Gas adsorption properties of the chromium-based metal organic framework MIL-101. J. Phys. Chem. C **2009**, 113, 6616-6621.
57. Llewellyn, P.L.;Bourrelly, S.;Serre, C.;Vimont, A.;Daturi, M.;Hamon, L.;De Weireld, G.;Chang, J.-S.;Hong, D.-Y.; Kyu Hwang, Y. High Uptakes of CO2 and CH4 in Mesoporous Metal® Organic Frameworks MIL-100 and MIL-101. Langmuir **2008**, 24, 7245-7250.
58. Elsayed, E.;Raya, A.-D.;Mahmoud, S.;Anderson, P.A.;Elsayed, A.; Youssef, P.G. CPO-27 (Ni), aluminium fumarate and MIL-101 (Cr) MOF materials for adsorption water desalination. Desalination **2017**, 406, 25-36.
59. Elsayed, A.;Al-Dadah, R.;Mahmoud, S.;Shi, B.;Youessef, P.;Elshaer, A.; Kaialy, W., Characterisation of CPO-27Ni Metal Organic Framework Material for Water Adsorption, in: Conference Paper, SusTEM, Newcastle University, UK, 2015.
60. Elsayed, E.;Raya, A.-D.;Mahmoud, S.;Elsayed, A.; Anderson, P.A. Aluminium fumarate and CPO-27 (Ni) MOFs: characterization and thermodynamic analysis for adsorption heat pump applications. Appl. Therm. Eng. **2016**, 99, 802-812.
61. Alvarez, E.;Guillou, N.;Martineau, C.;Bueken, B.;Van de Voorde, B.;Le Guillouzer, C.;Fabry, P.;Nouar, F.;Taulelle, F.; De Vos, D. The structure of the aluminum fumarate metal–organic framework A520. Angew. Chem. Int. Ed. **2015**, 54, 3664-3668.
62. Loiseau, T.;Serre, C.;Huguenard, C.;Fink, G.;Taulelle, F.;Henry, M.;Bataille, T.; Ferey, G. A rationale for the large breathing of the porous aluminum terephthalate (mil-53) upon hydration. Chem. Eur. J. **2004**, 10, 1373-1382.
63. Furukawa, H.;Gándara, F.;Zhang, Y.-B.;Jiang, J.;Queen, W.L.;Hudson, M.R.; Yaghi, O.M. Water adsorption in porous metal–organic frameworks and related materials. J. Am. Chem. Soc. **2014**, 136, 4369-4381.

64. De Lange, M.;Zeng, T.;Vlugt, T.;Gascon, J.; Kapteijn, F. Manufacture of dense CAU-10-H coatings for application in adsorption driven heat pumps: optimization and characterization. Cryst. Eng. Comm. **2015**, 17, 5911-5920.
65. Fröhlich, D.;Henninger, S.K.; Janiak, C. Multicycle water vapour stability of microporous breathing MOF aluminium isophthalate CAU-10-H. Dalton Trans. **2014**, 43, 15300-15304.
66. Fröhlich, D.;Pantatosaki, E.;Kolokathis, P.D.;Markey, K.;Reinsch, H.;Baumgartner, M.;van der Veen, M.A.;De Vos, D.E.;Stock, N.; Papadopoulos, G.K. Water adsorption behaviour of CAU-10-H: a thorough investigation of its structure–property relationships. J. Mater. Chem. A **2016**, 4, 11859-11869.
67. Hamon, L.;Serre, C.;Devic, T.;Loiseau, T.;Millange, F.;Férey, G.; Weireld, G.D. Comparative study of hydrogen sulfide adsorption in the MIL-53 (Al, Cr, Fe), MIL-47 (V), MIL-100 (Cr), and MIL-101 (Cr) metal− organic frameworks at room temperature. J. Am. Chem. Soc. **2009**, 131, 8775-8777.
68. Férey, G. Hybrid porous solids: past, present, future. Chem. Soc. Rev. **2008**, 37, 191-214.
69. Horcajada, P.;Surblé, S.;Serre, C.;Hong, D.-Y.;Seo, Y.-K.;Chang, J.-S.;Greneche, J.-M.;Margiolaki, I.; Férey, G. Synthesis and catalytic properties of MIL-100 (Fe), an iron (III) carboxylate with large pores. Chem. Commun. **2007**, 2820-2822.
70. Jeremias, F.;Khutia, A.;Henninger, S.K.; Janiak, C. MIL-100 (Al, Fe) as water adsorbents for heat transformation purposes—a promising application. Journal of Materials Chemistry **2012**, 22, 10148-10151.
71. Jasuja, H.;Zang, J.;Sholl, D.S.; Walton, K.S. Rational tuning of water vapor and CO2 adsorption in highly stable Zr-based MOFs. J. Phys. Chem. C **2012**, 116, 23526-23532.
72. Kim, S.-N.;Kim, J.;Kim, H.-Y.;Cho, H.-Y.; Ahn, W.-S. Adsorption/catalytic properties of MIL-125 and NH2-MIL-125. Catal. Today **2013**, 204, 85-93.
73. Chen, Y.-R.;Liou, K.-H.;Kang, D.-Y.;Chen, J.-J.; Lin, L.-C. Investigation of the Water Adsorption Properties and Structural Stability of MIL-100 (Fe) with Different Anions. Langmuir **2018**, 34, 4180-4187.
74. Kim, S.-I.;Yoon, T.-U.;Kim, M.-B.;Lee, S.-J.;Hwang, Y.K.;Chang, J.-S.;Kim, H.-J.;Lee, H.-N.;Lee, U.-H.; Bae, Y.-S. Metal–organic frameworks with high working capacities and cyclic hydrothermal stabilities for fresh water production. Chem. Eng. J. **2016**, 286, 467-475.
75. Wiersum, A.D.;Soubeyrand-Lenoir, E.;Yang, Q.;Moulin, B.;Guillerm, V.;Yahia, M.B.;Bourrelly, S.;Vimont, A.;Miller, S.; Vagner, C. An Evaluation of UiO-66 for Gas-Based Applications. Chem. Asian J. **2011**, 6, 3270-3280.
76. Tashiro, Y.;Kubo, M.;Katsumi, Y.;Meguro, T.; Komeya, K. Assessment of adsorption-desorption characteristics of adsorbents for adsorptive desiccant cooling system. Asian J. Mater. Sci. **2004**, 39, 1315-1319.
77. Meunier, F. Adsorption heat powered heat pumps. Appl. Therm. Eng. **2013**, 61, 830-836.
78. Bonaccorsi, L.;Calabrese, L.;Freni, A.;Proverbio, E.; Restuccia, G. Zeolites direct synthesis on heat exchangers for adsorption heat pumps. Appl. Therm. Eng. **2013**, 50, 1590-1595.
79. Garzón-Tovar, L.;Pérez-Carvajal, J.;Imaz, I.; Maspoch, D. Composite Salt in Porous Metal-Organic Frameworks for Adsorption Heat Transformation. Adv. Funct. Mater. **2017**, 27.
80. Yuan, Y.;Zhang, H.;Yang, F.;Zhang, N.; Cao, X. Inorganic composite sorbents for water vapor sorption: A research progress. Renewable Sustainable Energy Rev. **2016**, 54, 761-776.

81. Glaznev, I.;Ponomarenko, I.;Kirik, S.; Aristov, Y. Composites CaCl2/SBA-15 for adsorptive transformation of low temperature heat: Pore size effect. Int. J. Refrig. **2011**, 34, 1244-1250.
82. Petit, C.; Bandosz, T.J. Enhanced Adsorption of Ammonia on Metal-Organic Framework/Graphite Oxide Composites: Analysis of Surface Interactions. Adv. Funct. Mater. **2010**, 20, 111-118.
83. Yan, J.;Yu, Y.;Ma, C.;Xiao, J.;Xia, Q.;Li, Y.; Li, Z. Adsorption isotherms and kinetics of water vapor on novel adsorbents MIL-101 (Cr)@ GO with super-high capacity. Appl. Therm. Eng. **2015**, 84, 118-125.
84. Petit, C.;Burress, J.; Bandosz, T.J. The synthesis and characterization of copper-based metal–organic framework/graphite oxide composites. Carbon **2011**, 49, 563-572.
85. Yan, J.;Yu, Y.;Xiao, J.;Li, Y.; Li, Z. Improved Ethanol Adsorption Capacity and Coefficient of Performance for Adsorption Chillers of Cu-BTC@ GO Composite Prepared by Rapid Room Temperature Synthesis. Ind. Eng. Chem. Res. **2016**, 55, 11767-11774.
86. Elsayed, E.;Wang, H.;Anderson, P.A.;Al-Dadah, R.;Mahmoud, S.;Navarro, H.;Ding, Y.; Bowen, J. Development of MIL-101 (Cr)/GrO composites for adsorption heat pump applications. Microporous Mesoporous Mater. **2017**, 244, 180-191.
87. Mahanta, N.K.; Abramson, A.R., Thermal conductivity of graphene and graphene oxide nanoplatelets, in: Thermal and Thermomechanical Phenomena in Electronic Systems (ITherm), 2012 13th IEEE Intersociety Conference on, IEEE, 2012, pp. 1-6.
88. Zhou, K.;Mousavi, B.;Luo, Z.;Phatanasri, S.;Chaemchuen, S.; Verpoort, F. Characterization and properties of Zn/Co zeolitic imidazolate frameworks vs. ZIF-8 and ZIF-67. J. Mater. Chem. A **2017**, 5, 952-957.
89. Zhang, J.P.;Zhu, A.X.;Lin, R.B.;Qi, X.L.; Chen, X.M. Pore Surface Tailored SOD-Type Metal-Organic Zeolites. Adv. Mater. **2011**, 23, 1268-1271.
90. Birsa Čelič, T.;Mazaj, M.;Guillou, N.;Elkaïm, E.;El Roz, M.;Thibault-Starzyk, F.;Mali, G.;Rangus, M.;Čendak, T.; Kaučič, V.e. Study of hydrothermal stability and water sorption characteristics of 3-dimensional Zn-based trimesate. J. Phys. Chem. C **2013**, 117, 14608-14617.
91. Tatlıer, M.;Tantekin-Ersolmaz, B.; Erdem-Şenatalar, A. A novel approach to enhance heat and mass transfer in adsorption heat pumps using the zeolite–water pair. Microporous Mesoporous Mater. **1999**, 27, 1-10.
92. Bauer, J.;Herrmann, R.;Mittelbach, W.; Schwieger, W. Zeolite/aluminum composite adsorbents for application in adsorption refrigeration. Int. J. Energy Res. **2009**, 33, 1233-1249.
93. Bonaccorsi, L.;Freni, A.;Proverbio, E.;Restuccia, G.; Russo, F. Zeolite coated copper foams for heat pumping applications. Microporous Mesoporous Mater. **2006**, 91, 7-14.
94. Geus, E.R.;van Bekkum, H.;Bakker, W.J.; Moulijn, J.A. High-temperature stainless steel supported zeolite (MFI) membranes: preparation, module construction, and permeation experiments. Microporous Mater. **1993**, 1, 131-147.
95. Calabrese, L.;Bonaccorsi, L.;Freni, A.; Proverbio, E. Silicone composite foams for adsorption heat pump applications. Sustainable Mater.Technol. **2017**, 12, 27-34.
96. Calabrese, L.;Bonaccorsi, L.;Freni, A.; Proverbio, E. Synthesis of SAPO-34 zeolite filled macrocellular foams for adsorption heat pump applications: A preliminary study. Appl. Therm. Eng. **2017**, 124, 1312-1318.

97. Guilleminot, J.;Choisier, A.;Chalfen, J.;Nicolas, S.; Reymoney, J. Heat transfer intensification in fixed bed adsorbers. Heat Recovery Syst. CHP **1993**, 13, 297-300.